Progress in Fractional Differentiation and Applications
An International Journal

http://dx.doi.org/10.18576/pfda/100210

Fractional Approach for Belousov-Zhabotinsky Reactions Model with Unified Technique

Chandrali Baishya[1] *and Pundikala Veeresha*[2,*]

[1]Department of Studies and Research in Mathematics, Tumkur University, Tumkur-572103, India
[2]Center for Mathematical Needs, Department of Mathematics, CHRIST (Deemed to be University), Bengaluru - 560029, India

Received: 2 Sep. 2022, Revised: 18 Oct. 2022, Accepted: 28 Oct. 2022
Published online: 1 Apr. 2024

Abstract: The Belousov-Zhabotinsky reaction model represents chemical oscillators that exhibit periodic vibrations as a result of complex physic-chemical phenomena. The non-linear behaviour exhibited by Belousov-Zhabotinsky model is the cause of Turing patterns, birth of spiral waves, rise of limit cycle attractors, and deterministic chaos in many chemical reaction processes. Due to these noteworthy characteristics, in this paper, we have analyzed mathematical Belousov-Zhabotinsky model by a novel numerical approach q-Homotopy analysis transformation method. To interpret new observations, we have incorporated Caputo fractional derivative in the model. The numerical result are presented graphically and concerning the absolute error of solutions. With the help of the homotopy parameter curve, we have projected the convergence region with reference to diverse values of fractional derivative. This work establishes that the projected numerical algorithm is a well-organized tool to analyze the multifaceted coupled partial differential equation representing Belousov-Zhabotinsky type reactions.

Keywords: : Laplace transform; Caputo derivative; Belousov-Zhabotinsky system; q-Homotopy analysis method.

1 Introduction

When L'Hopital approached Leibniz somewhere in the year 1695 about the potential that n could be something other than an integer in $\frac{d^n f}{dt^n}$, the idea of fractional calculus was born. It sparked a debate on the matter that included notable mathematicians like Euler and Fourier. In 1730, a generalized law for calculating the derivative of a power function was introduced by Euler. Since then, many distinguished mathematicians have contributed to this field, including G. W. Leibniz, P. S. Laplace, J. Fourier, J. Liouville, B. Riemann, N. H. Abel, O. Heaviside, J. Hadamard , A. K. Grunwald, G. H. Hardy, H. J. Holmgren, A. V. Letnikov, M. Caputo, and others. As a result, many fractional derivatives, namely Grunwald-Letnikov, Riemann-Liouville, Caputo, Hadamard and other types have been introduced in the literature of fractional calculus [1–4]. However, for more than 200 years, fractional Calculus has been rarely taught as part of curricular, owing to the contradiction of several proposed definitions for fractional derivatives and the lack of practical applications. As a result, most scientists and engineers are unaware of the subject, while others are sceptical. Since past 45 years, the premise eventuated to change from pure mathematical analysis to applications in a variety of fields, as several applied scientists identified and demonstrated that integer-order differential operators are not adequate to symbolize physical properties such as long-range, random walk, non-Markovian processes, anomalous diffusion, and, most essentially, diversified behaviour. In order to precisely recreate the above-mentioned natural processes, the notion of non-local differential operators and local differential operators, in conjunction with the power-law setting was proposed. Oldham and Spanier [1], Miller and Ross [2], Kiryakova [3], Carpinteri and Mainardi [4], Podlubny [5], and Hilfer [6] Samko, Kilbas, and Srivastava [7], have all written books and monographs that have helped to introduce the field to the engineering, science, economics, and finance communities. As a result of continuous progress in this field, fractional calculus has made a reflective impression in the areas such as viscoelasticity and rheology [8], biology [9] signal and image processing [10], biophysics and bioengineering [11], physics [12], mechanics [13], earthquake [14, 15],

* Corresponding author e-mail: pundikala.veeresha@christuniversity.in

Finance [16], trafic model [17] and many others [18–20]. Even though fractional derivatives like Riemann-Liouville, Caputo have dominated this field for many decades, Caputo-Fabrizio [21, 22] and Atagnana- Baleanu [23–25] fractional derivatives in the presence of the non-singular kernel in them, have gained popularity in recent years.

Near the beginning of 1950s, Boris Belousov noticed that a solution of potassium bromate, citric acid, and cerium(IV) sulfate in dilute sulfuric acid did not react to equilibrium directly, instead it went colorless for a long time before returning to yellow. Since 1951, he had been trying to publish his work in peer-reviewed publications, but his findings had been denied because the reviewers believed that they violated the principle of thermodynamic equilibrium. Chemical oscillations were compared to a physical pendulum that defied the Second Law of Thermodynamics by swinging through equilibrium numerous times. Eight years later, in 1959, in a conference proceeding Belousov's work was ultimately published [26]. Anatol Zhabotinsky, a doctoral student working under Professor Schnoll's supervision, examined the reaction in depth in 1961 and was able to publish his findings [27]. Belousov-Zhabotinsky (BZ) reaction is the name of this temporally oscillating chemical reaction and this is amongst the most intriguing and well-documented chemical oscillators. Based on the method which Field et al. [28] had projected concerning the Belousov reaction, Field and Noyes proposed a five-step model:

$$\begin{aligned} &a+\mathscr{R}\rightarrow\mathscr{S}+p\\ &\mathscr{R}+\mathscr{S}\rightarrow p\\ &b+\mathscr{S}\rightarrow 2\mathscr{R}+Z\\ &2\mathscr{R}\rightarrow q\\ &Z\rightarrow f\mathscr{S} \end{aligned} \tag{1}$$

where $\mathscr{R}$, $\mathscr{S}$ and Z represent the concentration of the intermediaries bromous acid, bromate ion, and cerium IV respectively, p and q are products, and a and b are reactants. The model's product and reactant concentrations are kept constant, resulting in a functionally open system. By applying the law of mass action to reaction (1), the following differential equations characterizing the model's dynamics are produced :

$$\begin{aligned} \frac{d\mathscr{R}}{d\tau}&=\beta_1 a\mathscr{S}-\beta_2\mathscr{R}\mathscr{S}+\beta_3 b\mathscr{R}-2\beta_4\mathscr{R}^2,\\ \frac{d\mathscr{S}}{d\tau}&=-\beta_1 a\mathscr{S}-\beta_2\mathscr{R}\mathscr{S}+f\beta_3 Z,\\ \frac{dZ}{d\tau}&=\beta_3 b\mathscr{R}-\beta_5 Z. \end{aligned} \tag{2}$$

The forward rate constants for reaction (1) are denoted by $\beta_{\mathrm{i}}(\mathrm{i}=1,2,3,4,5)$ in Eq. (2). If in the model (2), it is assumed that the intermediaries $\mathscr{R},\mathscr{S},\mathrm{Z}$ can be diffused with constant diffusion coefficients say k_1,k_2,k_3, and then they are to be the functions of the spatial variables $\mathrm{x},\mathrm{y},\mathrm{z}$ and time variable t. Then model (2) takes the following form:

$$\begin{aligned} \frac{d\mathscr{R}}{d\tau}&=\beta_1 a\mathscr{S}-\beta_2\mathscr{R}\mathscr{S}+\beta_3 b\mathscr{R}-2\beta_4\mathscr{R}^2+\kappa_1\frac{\partial^2\mathscr{R}}{\partial\varkappa^2},\\ \frac{d\mathscr{S}}{d\tau}&=-\beta_1 a\mathscr{S}-\beta_2\mathscr{R}\mathscr{S}+f\beta_3 Z+\kappa_2\frac{\partial^2\mathscr{S}}{\partial\varkappa^2},\\ \frac{dZ}{d\tau}&=\beta_3 b\mathscr{R}-\beta_5 Z+\kappa_3\frac{\partial^2 Z}{\partial\varkappa^2}. \end{aligned} \tag{3}$$

Field and Noyes [29] noted that the concentration of cerium IV is zero in the foremost boundary of a wavefront of chemical activity and hence set $Z=0$ in (3) to suggest the following model:

$$\begin{aligned} \frac{d\mathscr{R}}{d\tau}&=\beta_1 a\mathscr{S}-\beta_2\mathscr{R}\mathscr{S}+\beta_3 b\mathscr{R}-2\beta_4\mathscr{R}^2+\kappa_1\frac{\partial^2\mathscr{R}}{\partial\varkappa},\\ \frac{d\mathscr{S}}{d\tau}&=-\beta_1 a\mathscr{S}-\beta_2\mathscr{R}\mathscr{S}+\kappa_2\frac{\partial^2\mathscr{S}}{\partial\varkappa^2}. \end{aligned} \tag{4}$$

Considering the multifaceted behaviour of the fractional differential equations (FDEs), many classical numerical techniques are modified to make them compatible for handling FDEs. They include Adomian decomposition method [30], He's variational iteration method [31], homotopy perturbation method [32], homotopy analysis method (HAM) [33], differential transform method [34], predictor-corrector approach [35], artificial neural network approach [36] and many others [37–39]. Because HAM [40] is used to solve nonlinear problems without transformation, linearization, and discretization, it needs large CPU time and computer memory. But combining HAM with

well-established transform resolves this issue. In order to reduce the large computation and computer memory, in this paper, we have considerd a modified version of HAM incorporating Laplace transform in it, named as q-homotopy analysis transform method (q-HATM) [41]. The considered algorithm is used to study numerous well-known nonlinear models because to its effectiveness and consistency, and the results show that the nature of the captured behaviour is exceptional [42, 43]. The proposed method is useful since it includes a convergence-control parameter that allows us to easily alter and have power over the region of convergence and speed of convergence of the approximation series. Due to this advantage, q-HATM is advanced in contrast to other analytic methods and perturbation techniques present in the literature. The BZ reaction model with a convenient form is presented as

$$\begin{aligned} \frac{\partial \mathscr{R}(\varkappa,\tau)}{\partial \tau} &= \kappa_1 \frac{\partial^2 \mathscr{R}}{d\varkappa^2} + \delta\alpha\mathscr{S} + \mathscr{R}(1-\mathscr{R}) - \alpha\mathscr{R}\mathscr{S}, \\ \frac{\partial \mathscr{S}(\varkappa,\tau)}{\partial \tau} &= \kappa_2 \frac{\partial^2 \mathscr{S}}{d\varkappa^2} + \gamma\mathscr{S} - \beta\mathscr{R}\mathscr{S}. \end{aligned} \tag{5}$$

Here, κ_1 and κ_2 are the diffusion constants for the concentration $\mathscr{R}$ and $\mathscr{S}$ respectively. Moreover, δ, γ are constants and α, $\beta \neq 1$ are positive parameters. To extract more information about the model, we have considered the equation (5) in the frame of Caputo fractional derivative and applied q-HATM to solve it. The fractional BZ equation is presented as:

$$\begin{aligned} D_t^{\mu}\mathscr{R}(\varkappa,\tau) &= \kappa_1 \frac{\partial^2 \mathscr{R}}{d\varkappa^2} + \delta\alpha\mathscr{S} + \mathscr{R}(1-\mathscr{R}) - \alpha\mathscr{R}\mathscr{S}, \\ D_t^{\mu}\mathscr{S}(\varkappa,\tau) &= \kappa_2 \frac{\partial^2 \mathscr{S}}{d\varkappa^2} + \gamma\mathscr{S} - \beta\mathscr{R}\mathscr{S}. \end{aligned} \tag{6}$$

This work is structured as follows: Section 2 contains the preliminary definitions corresponding to Caputo fractional derivative. The solution procedure of q-HATM is presented in Section 3. Then, the solutions for considered coupled system (6) under the influence of two different initial conditions are demonstrated using q-HATM method and presented their analysis graphically and error analysis in Section 4. Finally, we have produced the results and discussion in Section 5, followed by conclusion in Section 6.

2 Preliminaries

The basic definitions related to fractional calculus and LT are presented in this segment.

Definition 1(5). *The fractional Riemann-Liouville integral of a function* $f(t) \in C_{\delta}\,(\delta \geq -1)\,(\alpha > 0)$ *is defined as*

$$\begin{aligned} J^{\mu} f(t) &= \frac{1}{\Gamma(\mu)} \int_0^t (t-\vartheta)^{\mu-1} f(\vartheta)\, d\vartheta, \\ J^{0} f(t) &= f(t). \end{aligned} \tag{7}$$

Definition 2(5). *The Caputo fractional derivative for* $f \in H^1(a,\, b)$ *is presented as*

$$D_t^{\mu} f(t) = \begin{cases} \frac{d^n f(t)}{dt^n}, & \mu = n \in \mathbb{N}, \\ \frac{1}{\Gamma(n-\mu)} \int_0^t (t-\vartheta)^{n-\mu-1} f^{(n)}(\vartheta)\, d\vartheta, & n-1 < \mu < n\,, n \in \mathbb{N}. \end{cases} \tag{8}$$

Definition 3(5). *The LT of fractional Caputo derivative of* $f(t)$ *is*

$$L\left[D_t^{\mu} f(t)\right] = s^{\mu} F(s) - \sum_{r=0}^{n-1} s^{\alpha-r-1} f^{(r)}\left(0^{+}\right),\ (n-1 < \mu \leq n), \tag{9}$$

where $F(s)$ *is LT of* $f(t)$.

3 Solution Procedure of q-HATM

In this section, we hired the FDE to present the basic algorithm of the q-HATM scheme with initial conditions

$$D_t^{\mu} v(x,t) + \mathscr{R}\, v(x,t) + \mathscr{N} v(x,t) = f(x,t), \quad 0 < \mu \leq 1, \tag{10}$$

and

$$v(x,0) = g(x). \tag{11}$$

By employing LT on Eq. (10), then one can get

$$\mathscr{L}[v(x,t)] - \frac{g(x)}{s} + \frac{1}{s^{\mu}}\{\mathscr{L}[\mathscr{R}v(x,t)] + \mathscr{L}[\mathscr{N}\, v(x,t)] - \mathscr{L}[f(x,t)]\} = 0. \tag{12}$$

For $\varphi(x,t;q)$, $\mathscr{N}$ is contracted as follows

$$\mathscr{N}[\varphi(x,t;q)] = \mathscr{L}[\varphi(x,t;q)] - \frac{g(x)}{s} + \frac{1}{s^{\mu}}\{L[\mathscr{N}\varphi(x,t;q) + \mathscr{L}[\mathscr{R}\,\varphi(x,t;q)]] - L[f(x,t)]\}, \tag{13}$$

where $q \in \left[0, \frac{1}{n}\right]$. Now, the homotopy is presented as

$$(1-nq)\mathscr{L}[\varphi(x,\, t;q) - v_0(x,t)] = \hbar q \mathscr{N}[\varphi(x,\, t;q)], \tag{14}$$

then we have

$$\varphi(x,t;0) = v_0(x,t), \quad \varphi\left(x,t;\frac{1}{n}\right) = v(x,t). \tag{15}$$

Clearly, $\varphi(x,t;q)$changes from $v_0(x,t)$ to $v(x,t)$ when intensifying q from 0 to $\frac{1}{n}$. By using the Taylor theorem, we get

$$\varphi(x,t;q) = v_0(x,t) + \sum_{m=1}^{\infty} v_m(x,t)\, q^m, \tag{16}$$

where

$$v_m(x,t) = \frac{1}{m!}\frac{\partial^m \varphi(x,\, t;q)}{\partial q^m}|_{q=0}. \tag{17}$$

For the appropriate value of $v_0(x,t)$, Eq. (17) converges at $q = \frac{1}{n}$, n and $\hbar$. Then

$$v(x,t) = v_0(x,t) + \sum_{m=1}^{\infty} v_m(x,t)\left(\frac{1}{n}\right)^m. \tag{18}$$

After differentiating Eq. (14) m-times with q and multiplying by $\frac{1}{m!}$ and substituting $q = 0$, we have

$$\mathscr{L}[v_m(x,t) - k_m v_{m-1}(x,t)] = \hbar \Re_m(\overrightarrow{v}_{m-1}) \tag{19}$$

where

$$\overrightarrow{v}_m = \{v_0(x,t), v_1(x,t), \ldots, v_m(x,t)\}. \tag{20}$$

Eq. (19) simplifies after hiring inverse LT to

$$v_m(x,t) = k_m v_{m-1}(x,t) + \hbar \mathscr{L}^{-1}[\Re_m(\overrightarrow{v}_{m-1})]. \tag{21}$$

Here

$$\Re_m(\overrightarrow{v}_{m-1}) = L[v_{m-1}(x,t)] - \left(1 - \frac{k_m}{n}\right)\left(\frac{g(x)}{s} + \frac{1}{s^{\mu}}L[f(x,t)]\right) + \frac{1}{s^{\mu}}L[Rv_{m-1} + \mathscr{H}_{m-1}], \tag{22}$$

and

$$k_m = \begin{cases} 0, & m \le 1, \\ n, & m > 1. \end{cases} \tag{23}$$

In Eq. (22), $\mathscr{H}_m$ is homotopy polynomial and which is defined as

$$\mathscr{H}_m = \frac{1}{m!}\left[\frac{\partial^m \varphi(x,t;q)}{\partial q^m}\right]_{q=0} \text{ and } \varphi(x,t;q) = \varphi_0 + q\varphi_1 + q^2\varphi_2 + \ldots. \tag{24}$$

By using Eqs. (21) and (22), we have

$$v_m(x,t) = (k_m + \hbar)v_{m-1}(x,t) - \left(1 - \frac{k_m}{n}\right)\mathscr{L}^{-1}\left(\frac{g(x)}{s} + \frac{1}{s^{\mu}}L[f(x,t)]\right) + \hbar\mathscr{L}^{-1}\left\{\frac{1}{s^{\mu}}L[Rv_{m-1} + \mathscr{H}_{m-1}]\right\}. \tag{25}$$

By the help of q-HATM, the series solution is

$$v(x,t) = v_0(x,t) + \sum_{m=1}^{\infty} v_m(x,t). \tag{26}$$

4 Solution for the Considered Coupled System

In this section, we have considered Eq. (6) subject to different initial conditions and solved them with the help of q-HATM. The obtained results are projected graphically and in tabular form.

Example 1.

$$D_t^{\mu}\mathscr{R}(\varkappa,\tau)-\frac{\partial^2\mathscr{R}}{d\varkappa^2}-\alpha\mathscr{S}-\mathscr{R}+\mathscr{R}^2+\alpha\mathscr{R}\mathscr{S}=0,$$
$$D_t^{\mu}\mathscr{S}(\varkappa,\tau)-\frac{\partial^2\mathscr{S}}{d\varkappa^2}-\beta\mathscr{S}+\beta\mathscr{R}\mathscr{S}=0, \tag{27}$$

with initial conditions

$$\mathscr{R}(\varkappa,0)=\frac{1}{\left(e^{\sqrt{\frac{\beta}{6}}\varkappa}+1\right)^2},\ \mathscr{S}(\varkappa,0)=\frac{\beta-1}{\alpha\left(e^{\sqrt{\frac{\beta}{6}}\varkappa}+1\right)^2}. \tag{28}$$

Taking LT on Eq. (27) and then using the Eq. (28), we get

$$L[\mathscr{R}(\varkappa,\tau)]-\frac{1}{s}\left(\frac{1}{\left(e^{\sqrt{\frac{\beta}{6}}\varkappa}+1\right)^2}\right)-\frac{1}{s^{\mu}}L\left\{\frac{\partial^2\mathscr{R}}{d\varkappa^2}+\alpha\mathscr{S}+\mathscr{R}-\mathscr{R}^2-\alpha\mathscr{R}\mathscr{S}\right\}=0,$$
$$L[\mathscr{S}(\varkappa,\tau)]-\frac{1}{s}\left(\frac{\beta-1}{\alpha\left(e^{\sqrt{\frac{\beta}{6}}\varkappa}+1\right)^2}\right)-\frac{1}{s^{\mu}}L\left\{\frac{\partial^2\mathscr{S}}{d\varkappa^2}+\beta\mathscr{S}-\beta\mathscr{R}\mathscr{S}\right\}=0. \tag{29}$$

The non-linear operator N is presented with the help of future algorithm as below

$$\begin{aligned}N^1[\varphi_1(\varkappa,\tau;q),\ \varphi_2(\varkappa,\tau;q)]&=L[\varphi_1(\varkappa,\tau;q)]-\frac{1}{s}\left(\frac{1}{\left(e^{\sqrt{\frac{\beta}{6}}\varkappa}+1\right)^2}\right)\\&-\frac{1}{s^{\mu}}L[\frac{\partial^2\varphi_1(\varkappa,\tau;q)}{d\varkappa^2}+\alpha\varphi_2(\varkappa,\tau;q)+\varphi_1(\varkappa,\tau;q)-\varphi_1^2(\varkappa,\tau;q)\\&-\alpha\varphi_1(\varkappa,\tau;q)\varphi_2(\varkappa,\tau;q)],\\N^2[\varphi_1(\varkappa,\tau;q),\ \varphi_2(\varkappa,\tau;q)]&=L[\varphi_2(\varkappa,\tau;q)]-\frac{1}{s}\left(\frac{\beta-1}{\alpha\left(e^{\sqrt{\frac{\beta}{6}}\varkappa}+1\right)^2}\right)\\&-\frac{1}{s^{\mu}}L\left[\frac{\partial^2\varphi_2(\varkappa,\tau;q)}{d\varkappa^2}+\beta\varphi_2(\varkappa,\tau;q)-\beta\varphi_1(\varkappa,\tau;q)\varphi_2(\varkappa,\tau;q)\right].\end{aligned} \tag{30}$$

The deformation equation of m order by the help of q-HATM at $\mathscr{H}(\varkappa,\tau)=1$, is given as follows

$$L[\mathscr{R}_m(\varkappa,\tau)-k_m\mathscr{R}_{m-1}(\varkappa,\tau)]=\hbar\mathfrak{R}_{1,m}\left[\overrightarrow{\mathscr{R}}_{m-1},\overrightarrow{\mathscr{S}}_{m-1}\right],$$
$$L[\mathscr{S}_m(\varkappa,\tau)-k_m v_{m-1}(\varkappa,\tau)]=\hbar\mathfrak{R}_{2,m}\left[\overrightarrow{\mathscr{R}}_{m-1},\overrightarrow{\mathscr{S}}_{m-1}\right], \tag{31}$$

where

$$\Re_{1,m}\left[\overrightarrow{\mathscr{R}}_{m-1},\overrightarrow{\mathscr{S}}_{m-1}\right]=L[\mathscr{R}_{m-1}(\varkappa,\tau)]-\left(1-\frac{k_m}{n}\right)\frac{1}{s}\frac{1}{\left(e^{\sqrt{\frac{\beta}{6}}\varkappa}+1\right)^2}$$
$$-\frac{1}{s^\mu}L\left[\frac{\partial^2\mathscr{R}_{m-1}}{d\varkappa^2}+\alpha\mathscr{S}_{m-1}+\mathscr{R}_{m-1}-\sum_{i=0}^{m-1}\mathscr{R}_i\mathscr{R}_{m-1-i}-\alpha\sum_{i=0}^{m-1}\mathscr{R}_i\mathscr{S}_{m-1-i}\right],$$
$$\Re_{2,m}\left[\overrightarrow{\mathscr{R}}_{m-1},\overrightarrow{\mathscr{S}}_{m-1}\right]=L[\mathscr{S}_{m-1}(\varkappa,\tau)]-\left(1-\frac{k_m}{n}\right)\frac{1}{s}\frac{\beta-1}{\alpha\left(e^{\sqrt{\frac{\beta}{6}}\varkappa}+1\right)^2}$$
$$+\frac{1}{s^\mu}L\left[\frac{\partial^2\mathscr{S}_{m-1}}{d\varkappa^2}+\beta\mathscr{S}_{m-1}-\beta\sum_{i=0}^{m-1}\mathscr{R}_i\mathscr{S}_{m-1-i}\right]. \tag{32}$$

On applying inverse LT on Eq. (31), it reduces to

$$\mathscr{R}_m(\varkappa,\tau)=k_m\mathscr{R}_{m-1}(\varkappa,\tau)+\hbar L^{-1}\left[\Re_{1,m}\left[\overrightarrow{\mathscr{R}}_{m-1},\overrightarrow{\mathscr{S}}_{m-1}\right]\right],$$
$$\mathscr{S}_m(\varkappa,\tau)=k_m\mathscr{S}_{m-1}(\varkappa,\tau)+\hbar L^{-1}\left[\Re_{2,m}\left[\overrightarrow{\mathscr{R}}_{m-1},\overrightarrow{\mathscr{S}}_{m-1}\right]\right]. \tag{33}$$

On simplifying the above equation systematically by using $\mathscr{R}_0(\varkappa,\tau)=\frac{1}{\left(e^{\sqrt{\frac{\beta}{6}}\varkappa}+1\right)^2}$ and $\mathscr{S}_0(\varkappa,\tau)=\frac{\beta-1}{\alpha\left(e^{\sqrt{\frac{\beta}{6}}\varkappa}+1\right)^2}$ we obtained the terms of the series solution

$$\mathscr{R}(\varkappa,\tau)=\mathscr{R}_0(\varkappa,\tau)+\sum_{m=1}^{\infty}\mathscr{R}_m(\varkappa,\tau)\left(\frac{1}{n}\right)^m,$$
$$\mathscr{S}(\varkappa,\tau)=\mathscr{S}_0(\varkappa,\tau)+\sum_{m=1}^{\infty}\mathscr{S}_m(\varkappa,\tau)\left(\frac{1}{n}\right)^m. \tag{34}$$

The corresponding exact solution for Eq. (27) is $\mathscr{R}(\varkappa,\tau)=\frac{e^{\frac{5\beta}{2}\tau}}{\left(e^{\sqrt{\frac{\beta}{6}}\varkappa}+e^{\frac{5\beta}{2}\tau}\right)^2}$ and $\mathscr{S}(\varkappa,\tau)=\frac{(\beta-1)e^{\frac{5\beta}{2}\tau}}{\alpha\left(e^{\sqrt{\frac{\beta}{6}}\varkappa}+e^{\frac{5\beta}{2}\tau}\right)^2}$.

Example 2.

$$D_t^\mu\mathscr{R}(\varkappa,\tau)-\frac{\partial^2\mathscr{R}}{d\varkappa^2}-\mathscr{R}+\mathscr{R}^2+\alpha\mathscr{R}\mathscr{S}=0,$$
$$D_t^\mu\mathscr{S}(\varkappa,\tau)-\frac{\partial^2\mathscr{S}}{d\varkappa^2}+\beta\mathscr{R}\mathscr{S}=0, \tag{35}$$

with initial conditions

$$\mathscr{R}(\varkappa,0)=\frac{1}{\left(e^{\sqrt{\frac{\beta}{6}}\varkappa}+1\right)^2},\ \mathscr{S}(\varkappa,0)=\frac{(1-\beta)e^{\sqrt{\frac{\beta}{6}}\varkappa}\left(e^{\sqrt{\frac{\beta}{6}}\varkappa}+2\right)}{\alpha\left(e^{\sqrt{\frac{\beta}{6}}\varkappa}+1\right)^2}. \tag{36}$$

Taking LT on Eq. (35) and then using the Eq. (36), we get

$$\mathrm{L}\left[\mathscr{R}\left(\varkappa,\tau\right)\right]-\frac{1}{s}\left(\frac{1}{\left(e^{\sqrt{\frac{\beta}{6}}\varkappa}+1\right)^{2}}\right)-\frac{1}{s^{\mu}}L\left[\frac{\partial^{2}\mathscr{R}}{d\varkappa^{2}}+\mathscr{R}-\mathscr{R}^{2}-\alpha\mathscr{R}\mathscr{S}\right]=0,$$

$$L\left[\mathscr{S}\left(\varkappa,\tau\right)\right]-\frac{1}{s}\left(\frac{(1-\beta)e^{\sqrt{\frac{\beta}{6}}\varkappa}\left(e^{\sqrt{\frac{\beta}{6}}\varkappa}+2\right)}{\alpha\left(e^{\sqrt{\frac{\beta}{6}}\varkappa}+1\right)^{2}}\right)-\frac{1}{s^{\mu}}L\left[\frac{\partial^{2}\mathscr{S}}{d\varkappa^{2}}-\beta\mathscr{R}\mathscr{S}\right]=0. \tag{37}$$

The non-linear operator N is presented with the help of future algorithm as below

$$N^{1}\left[\varphi_{1}\left(\varkappa,\tau;q\right),\ \varphi_{2}\left(\varkappa,\tau;q\right)\right]=L\left[\varphi_{1}\left(\varkappa,\tau;q\right)\right]-\frac{1}{s}\left(\frac{1}{\left(e^{\sqrt{\frac{\beta}{6}}\varkappa}+1\right)^{2}}\right)$$
$$-\frac{1}{s^{\mu}}L\left[\frac{\partial^{2}\varphi_{1}\left(\varkappa,\tau;q\right)}{d\varkappa^{2}}+\varphi_{1}\left(\varkappa,\tau;q\right)-\ \varphi_{1}^{2}\left(\varkappa,\tau;q\right)-\alpha\varphi_{1}\left(\varkappa,\tau;q\right)\varphi_{2}\left(\varkappa,\tau;q\right)\right]$$

$$N^{2}\left[\varphi_{1}\left(\varkappa,\tau;q\right),\ \varphi_{2}\left(\varkappa,\tau;q\right)\right]=L\left[\varphi_{2}\left(\varkappa,\tau;q\right)\right]-\frac{1}{s}\left(\frac{(1-\beta)e^{\sqrt{\frac{\beta}{6}}\varkappa}\left(e^{\sqrt{\frac{\beta}{6}}\varkappa}+2\right)}{\alpha\left(e^{\sqrt{\frac{\beta}{6}}\varkappa}+1\right)^{2}}\right)$$
$$-\frac{1}{s^{\mu}}L\left[\frac{\partial^{2}\varphi_{2}\left(\varkappa,\tau;q\right)}{d\varkappa^{2}}-\beta\varphi_{1}\left(\varkappa,\tau;q\right)\varphi_{2}\left(\varkappa,\tau;q\right)\right]. \tag{38}$$

Then, we have by Eq. (27)

$$\mathfrak{R}_{1,m}\left[\overrightarrow{\mathscr{R}}_{m-1},\ \overrightarrow{\mathscr{S}}_{m-1}\right]=L\left[\mathscr{R}_{m-1}\left(\varkappa,\tau\right)\right]-\left(1-\frac{k_{m}}{n}\right)\frac{1}{s}\left\{\frac{1}{\left(e^{\sqrt{\frac{\beta}{6}}\varkappa}+1\right)^{2}}\right\}$$
$$-\frac{1}{s^{\mu}}L\left[\frac{\partial^{2}\mathscr{R}_{m-1}}{d\varkappa^{2}}+\alpha\mathscr{S}_{m-1}+\mathscr{R}_{m-1}-\sum_{i=0}^{m-1}\mathscr{R}_{i}\mathscr{R}_{m-1-i}-\alpha\sum_{i=0}^{m-1}\mathscr{R}_{i}\mathscr{S}_{m-1-i}\right]$$

$$\mathfrak{R}_{2,m}\left[\overrightarrow{\mathscr{R}}_{m-1},\ \overrightarrow{\mathscr{S}}_{m-1}\right]=L\left[\mathscr{S}_{m-1}\left(\varkappa,\tau\right)\right]-\left(1-\frac{k_{m}}{n}\right)\frac{1}{s}\left\{\frac{(1-\beta)e^{\sqrt{\frac{\beta}{6}}\varkappa}\left(e^{\sqrt{\frac{\beta}{6}}\varkappa}+2\right)}{\alpha\left(e^{\sqrt{\frac{\beta}{6}}\varkappa}+1\right)^{2}}\right\}$$
$$+\frac{1}{s^{\mu}}L\left[\frac{\partial^{2}\mathscr{S}_{m-1}}{d\varkappa^{2}}+\beta\mathscr{S}_{m-1}-\beta\sum_{i=0}^{m-1}\mathscr{R}_{i}\mathscr{S}_{m-1-i}\right]. \tag{39}$$

On simplifying the above equation systematically by using

$$\mathscr{R}_{0}\left(\varkappa,\tau\right)=\frac{1}{\left(e^{\sqrt{\frac{\beta}{6}}\varkappa}+1\right)^{2}}\ \textit{and}\ \mathscr{S}_{0}\left(\varkappa,\tau\right)=\frac{(1-\beta)e^{\sqrt{\frac{\beta}{6}}\varkappa}\left(e^{\sqrt{\frac{\beta}{6}}\varkappa}+2\right)}{\alpha\left(e^{\sqrt{\frac{\beta}{6}}\varkappa}+1\right)^{2}}, \tag{40}$$

we obtained the terms of the series solution. The corresponding exact solution for Eq. (35) is

$$\mathscr{R}(\varkappa,\tau)=\frac{e^{\frac{5\beta}{3}\tau}}{\left(e^{\sqrt{\frac{\beta}{6}}\varkappa}+e^{\frac{5\beta}{3}\tau}\right)^2}$$

and

$$\mathscr{S}(\varkappa,\tau)=\frac{(1-\beta)e^{\sqrt{\frac{\beta}{6}}\varkappa}\left(e^{\sqrt{\frac{\beta}{6}}\varkappa}+2e^{\frac{5\beta}{3}\tau}\right)}{\alpha\left(e^{\sqrt{\frac{\beta}{6}}\varkappa}+e^{\frac{5\beta}{3}\tau}\right)^2}$$

.

5 Numerical Results and Discussion

This section presents an analysis of the numerical results obtained in Section 4 for the solution of the BZ model within the framework of Caputo fractional derivative using q-HATM. Graphical representations of solution curves of concentration $\mathscr{R}(\varkappa,\tau)$ and $\mathscr{S}(\varkappa,\tau)$ in spatio-temporal context give very interesting observations. Fig. 1 and Fig. 4 give the 3D representation of the comparison of q-HATM solutions with exact solutions for $\mu=1$ corresponding to Example 1 and Example 2 respectively. These profiles agree with the 2D profile projected in Fig. 2 and Fig. 5 for $\mu=1$. In Fig. 2(a), when $\tau=0.1$, for different values of μ, it is observed that the distribution of the concentrations $\mathscr{R}(\varkappa,\tau)$and $\mathscr{S}(\varkappa,\tau)$ continue to decrease monotonically in the region to the right of the expanding pulse of $\varkappa$. In Fig. 2(b), even though for $\mu=1$ and $\mu=0.75$, concentration distribution is monotonic, but for $\mu=0.5$ we observe the formulation of a new front. In Fig. 2(c), the monotonicity of concentration distributions are lost even for $\mu=0.75$, and two new fronts appear distinctively. In Fig. 2(d) and 2(e), the monotonic decreasing behaviour of the concentration distribution is completely disappeared and we can observe prominent development of new fronts with decreasing fractional-order μ and increasing temporal variable τ. A similar type of development from monotonically decreasing profile to oscillatory behaviour can be noticed in the graphical representation of solutions of Example 2 in Fig. 5. This observation clearly indicates that μ and τ prompt the oscillation of concentration distributions. To find the convergence region of the homotopy parameter $\hbar$ for different values of $\varkappa,\tau$ and n, we have sketched Fig. 3 and Fig. 6 for Example 1 and Example 2, respectively. In these figures, the interval in which the values of $\mathscr{R}(\varkappa,\tau)$and $\mathscr{S}(\varkappa,\tau)$ remain constant at particular values of $\varkappa$, τ and n are depicted. We decide a valid region as the region where the graphs of $\mathscr{R}(\varkappa,\tau)$and $\mathscr{S}(\varkappa,\tau)$ are parallel to the horizontal–axis ($\hbar$), since it allows us to easily change and regulate the speed of convergence of the series solution. From these figures, we notice that for the various values of $\varkappa,\tau$ and n, the valid intersection region of $\hbar$ becomes larger for $n=1$. In Fig. 3(a), when $n=1$, we observe that convergence region is $-1.5<\hbar<-1.6$ for $\mu=1$, $-1.1<\hbar<-0.5$ for $\mu=0.75$, and $-0.7<\hbar<-0.6$. Whereas, in Fig. 3(b), when $n=2$, the convergence region becomes smaller and commonly we notice that for different values of μ, $\hbar=-1$ can give better convergence to the solution. Similar behaviour of the variation of convergence region can be observed in Figure 6 corresponding to solutions of Example 2. The absolute errors presented in Tables 1 and 2 for the solutions of Example 1 and in Tables 3 for the solutions of Example 2 respectively, reveal that accuracy is higher with increasing $\varkappa$.

6 Conclusion

In this paper, the BZ equation describing chemical oscillators that exhibit periodic vibrations is considered incorporating Caputo fractional derivative. The approximate solution of the fractional BZ model is computed by means of the q-HATM method. The projected approach combines two efficient and classical techniques, HAM and LT, to overcome the limitations of most series solution methods in terms of convergence, as it does not necessitate discretization, perturbations, the formulation of a base function, or the conversion of the partial to ordinary differential equations. Because the present technique allows for the selection of homotopy parameters, we can produce results that quickly converge to the analytical solution when the homotopy parameter is selected correctly. In addition, the fractional operator under consideration aids in the capturing of more intriguing implications connected with hereditary and non-local features. Numerical simulation of the BZ model demonstrates the converges of q-HATM solution to the exact solution as the fractional order approaches the classical order. The findings show that the fractional operator under investigation and the strategy are pretty systematic and may be used to analyze the wide range of real-world models.

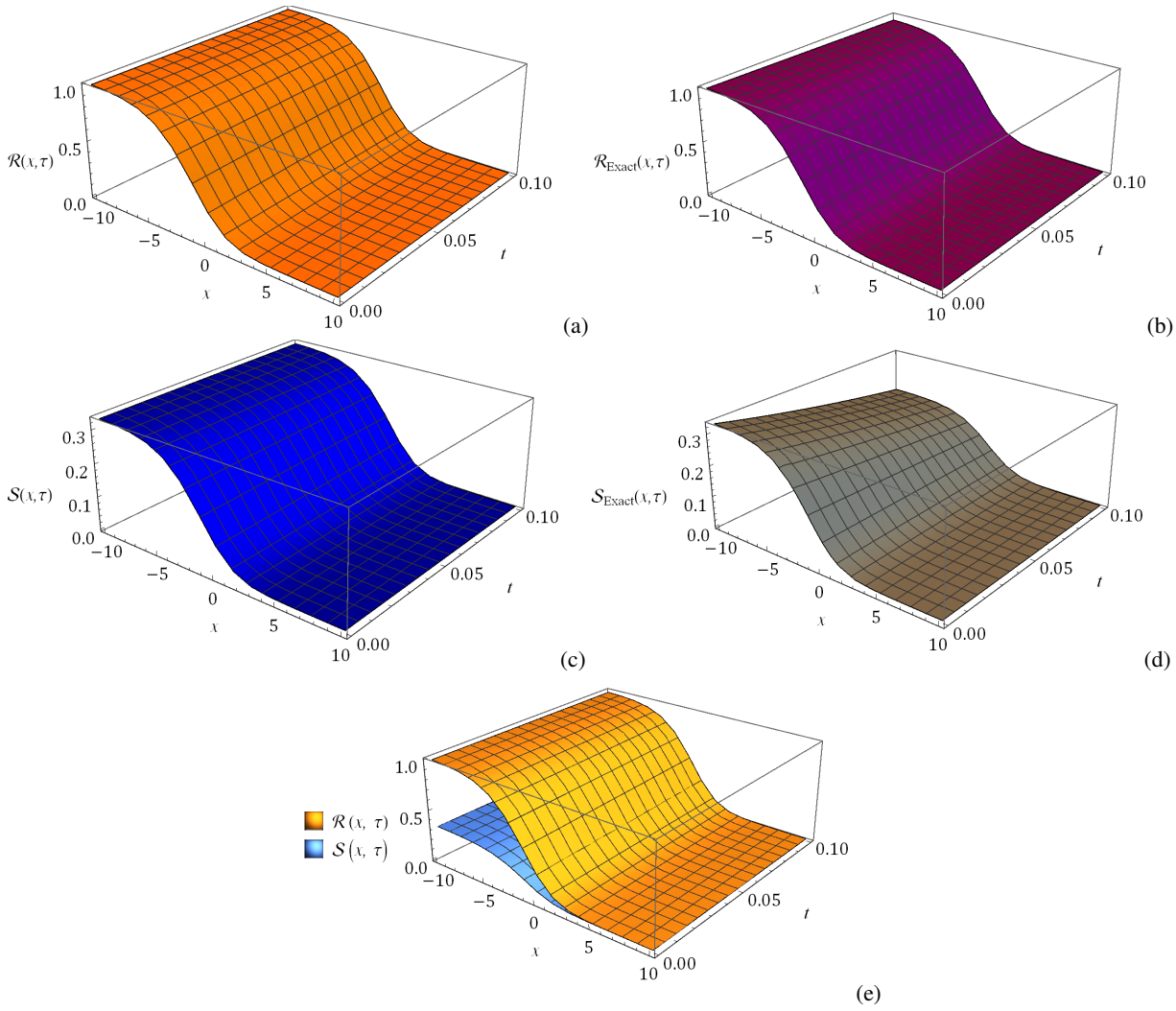

Fig. 1: Surfaces of $(a)\mathscr{R}_{q-HATM}$, $(b)\mathscr{R}_{Exact}$ $(c)\mathscr{S}_{q-HATM}$,$(d)\mathscr{S}_{Exact}$,(e) coupled surface at $\alpha = 2, \beta = 3,\ \hbar = -1,\ n = 1$ and $\mu = 1$ for Example 1.

References

[1] K. Oldham and J. Spanier, *The fractional calculus*, Academic Press, New York, 1974.
[2] K. S. Miller and B. Ross, *An introduction to fractional calculus and fractional differential equations*, A Wiley, New York, 1993.
[3] V. S. Kiryakova, *Generalized fractional calculus and applications*, Pitman Research Notes in Mathematics, vol. 301, Longman Sci. Tech. & J. Wiley, 1994.
[4] F. Mainardi, *Fractional calculus: some basic problems in continuum and statistical mechanics*. In: Fractals and Fractional Calculus in Continuum Mechanics (Eds. A. Carpinteri and F. Mainardi), Springer Verlag, Wien, 1997.
[5] I. Podlubny, *Fractional differential equations*, Academic Press, New York, 1999.
[6] R. Hilfer, *Applications of fractional calculus in physics*, World Scientific Publishing Company, 2000.
[7] A. A. Kilbas, H. M. Srivastava and J. J. Trujillo, *Theory and applications of fractional differential equations*, Elsevier, Amsterdam, 2006.
[8] D. Craiem and R. L. Armentano, A fractional derivative model to describe arterial viscoelasticity, *Biorheology* **44**, 251–263 (2007).
[9] C. Baishya, S. J. Achar, P. Veeresha and D. G. Prakasha, Dynamics of a fractional epidemiological model with disease infection in both the populations, *Chaos* **31**(4), (2021).
[10] R. L. Magin, *Fractional calculus in bioengineering*, Begell House, Connecticut, 2006.
[11] M. D. Ortigueira, On the initial conditions in continuous-time fractional linear systems, *Signal Proc.* **83**(11), 2301-2309 (2003).
[12] Y. A. Rossikhin and M. V. Shitikova, Applications of fractional calculus to dynamic problems of linear and nonlinear hereditary mechanics of solids, *Appl. Mech. Rev.* **63**(1), (2010).

Table 1: Analysis for different μ at distinct $\varkappa$ andτ for $\mathscr{R}(\varkappa,\tau)$ of Example 1 with $\alpha=2,\ \beta=3,\ n=1$ and $\hbar=-1$.

$\varkappa$	τ	$\mu=0.7$	$\mu=0.8$	$\mu=0.9$	$\mu=1$
5	0.02	5.28868×10^{-4}	3.62897×10^{-4}	2.40514×10^{-4}	1.54149×10^{-4}
	0.04	7.86481×10^{-4}	5.88650×10^{-4}	4.25982×10^{-4}	2.98035×10^{-4}
	0.06	9.76537×10^{-4}	7.66905×10^{-4}	5.85259×10^{-4}	4.32290×10^{-4}
	0.08	1.13259×10^{-3}	9.16006×10^{-4}	7.25530×10^{-4}	5.57549×10^{-4}
	0.10	1.27010×10^{-3}	1.04532×10^{-3}	8.50888×10^{-4}	6.74446×10^{-4}
10	0.02	1.89449×10^{-6}	1.30306×10^{-6}	8.64578×10^{-7}	5.53798×10^{-7}
	0.04	2.80634×10^{-6}	2.10377×10^{-6}	1.52516×10^{-6}	1.06762×10^{-6}
	0.06	3.48227×10^{-6}	2.73220×10^{-6}	2.08840×10^{-6}	1.54426×10^{-6}
	0.08	4.04695×10^{-6}	3.25743×10^{-6}	2.58170×10^{-6}	1.98654×10^{-6}
	0.10	4.55833×10^{-6}	3.71527×10^{-6}	3.02105×10^{-6}	2.39724×10^{-6}
15	0.02	5.93766×10^{-9}	4.08456×10^{-9}	2.71029×10^{-9}	1.73600×10^{-9}
	0.04	8.79374×10^{-9}	6.59272×10^{-9}	4.77999×10^{-9}	3.34612×10^{-9}
	0.06	1.09117×10^{-8}	8.56055×10^{-9}	6.54394×10^{-9}	4.83923×10^{-9}
	0.08	1.26831×10^{-8}	1.02053×10^{-8}	8.08842×10^{-9}	6.22422×10^{-9}
	0.10	1.42902×10^{-8}	1.16396×10^{-8}	9.46373×10^{-9}	7.50998×10^{-9}

Table 2: Analysis for different μ at distinct $\varkappa$ and $\tau$for$\mathscr{S}(\varkappa,\tau)$ of Example 1 with $\alpha=2,\ \beta=3,\ n=1,\ \hbar=-1$.

$\varkappa$	τ	$\mu=0.7$	$\mu=0.8$	$\mu=0.9$	$\mu=1$
5	0.02	1.52804×10^{-4}	6.34298×10^{-5}	2.59498×10^{-5}	8.50690×10^{-6}
	0.04	2.39716×10^{-4}	9.67811×10^{-5}	5.51216×10^{-5}	5.06559×10^{-6}
	0.06	3.11880×10^{-4}	1.21698×10^{-4}	8.78071×10^{-5}	3.56407×10^{-6}
	0.08	3.74717×10^{-4}	1.40690×10^{-4}	1.24258×10^{-4}	1.65971×10^{-5}
	0.10	4.30068×10^{-4}	1.54544×10^{-4}	1.64670×10^{-4}	3.38494×10^{-5}
10	0.02	5.41692×10^{-7}	2.12390×10^{-7}	1.14575×10^{-7}	1.11635×10^{-8}
	0.04	8.40327×10^{-7}	3.09486×10^{-7}	2.49695×10^{-7}	2.88579×10^{-8}
	0.06	1.07647×10^{-6}	3.66217×10^{-7}	4.08893×10^{-7}	9.83462×10^{-8}
	0.08	1.26603×10^{-6}	3.88301×10^{-7}	5.96051×10^{-7}	1.97568×10^{-7}
	0.10	1.41173×10^{-6}	3.74804×10^{-7}	8.15429×10^{-7}	3.29493×10^{-7}
15	0.02	1.69682×10^{-9}	6.63034×10^{-10}	3.62983×10^{-10}	3.15297×10^{-11}
	0.04	2.63049×10^{-9}	9.63250×10^{-10}	7.92098×10^{-10}	9.89900×10^{-11}
	0.06	3.36635×10^{-9}	1.13493×10^{-9}	1.29896×10^{-9}	3.24030×10^{-10}
	0.08	3.95354×10^{-9}	1.19527×10^{-9}	1.89640×10^{-9}	6.45109×10^{-10}
	0.10	4.39966×10^{-9}	1.14048×10^{-9}	2.59859×10^{-9}	1.07237×10^{-9}

[13] J. M. Sabatier, O. P. Agrawal and J. A. T. Machado, *Advances in fractional calculus: theoretical developments and applications in physics and engineering*, Springer, Berlin, 2007.

[14] C. G. Koh and J. M. Kelly, Application of fractional derivatives to seismic analysis of based isolated models, *Earth. Eng. Struct. Dyn.* **19**, 229-241 (1990).

Table 3: Comparison of the iterative terms for the obtained results for Example 2 with distinct $\varkappa$ and τ at $\alpha = 2,\ \beta = 3,\ n = 1,\ \hbar = -1$ and $\mu = 1$.

$\varkappa$	τ	$\lvert\mathscr{R}_{Exact} - \mathscr{R}^{(2)}_{q-HATM}\rvert$	$\lvert\mathscr{R}_{Exact} - \mathscr{R}^{(3)}_{q-HATM}\rvert$	$\lvert\mathscr{S}_{Exact} - \mathscr{S}^{(2)}_{q-HATM}\rvert$	$\lvert\mathscr{S}_{Exact} - \mathscr{S}^{(3)}_{q-HATM}\rvert$
5	0.025	2.07951×10^{-4}	1.44679×10^{-5}	7.57360×10^{-5}	1.22654×10^{-5}
	0.050	4.33898×10^{-4}	3.73840×10^{-5}	1.57943×10^{-4}	2.67277×10^{-5}
	0.075	6.79078×10^{-4}	6.53005×10^{-5}	2.45897×10^{-4}	4.36166×10^{-5}
	0.100	9.44730×10^{-4}	9.75792×10^{-5}	3.38222×10^{-4}	6.31662×10^{-5}
10	0.025	7.51165×10^{-7}	8.91544×10^{-8}	1.46297×10^{-7}	7.87897×10^{-8}
	0.050	1.56786×10^{-6}	1.86755×10^{-7}	3.26050×10^{-7}	2.01776×10^{-7}
	0.075	2.45007×10^{-6}	2.93455×10^{-7}	5.46414×10^{-7}	3.61341×10^{-7}
	0.100	3.39780×10^{-6}	4.09908×10^{-7}	8.15429×10^{-7}	5.61303×10^{-7}

[15] J. He, Nonlinear oscillation with fractional derivative and its applications, Conference on Vibrating Engineering, Dalian, China, (1998), 288-291.

[16] R. Baillie, Long memory processes and fractional integration in econometrics, *J. Econometrics*, 73(1) (1996), 5-59.

[17] J. He, Some applications of nonlinear fractional differential equations and their approximations, *Bull. Sci. Tech. Soc.* **15**, 86-90 (1999).

[18] P. Veeresha, E. Ilhan and H. M. Baskonus, Fractional approach for analysis of the model describing wind-influenced projectile motion, *Phys. Scripta* **96** (7), 075209 (2021).

[19] W. Gao, et al., Modified predictor-corrector method for the numerical solution of a fractional-order SIR model with 2019-nCoV, *Fract. Fraction.* **6**(2), (2022).

[20] P. Veeresha, H. M. Baskonus and W. Gao, Strong interacting internal waves in rotating ocean: Novel fractional approach, *Axioms* **10**(2), 123 (2021).

[21] M. Caputo and M. Fabrizio, A new definition of fractional derivative without singular kernel, *Progr. Fract. Differ. Appl.* **1**, 73-85 (2015).

[22] A. Atangana and D. Baleanu, Caputo-Fabrizio derivative applied to groundwater flow within conned aquifer, *J. Eng. Mech.* **143**(5), (2017).

[23] A. Atangana and D. Baleanu, New fractional derivatives with nonlocal and non-singular kernel: theory and application to heat transfer model, *Therm. Sci.* **20**(2), 763-769 (2016).

[24] A. Atangana and I. Koca, Chaos in a simple nonlinear system with Atangana-Baleanu derivatives with fractional order, *Chaos Solit. Fract.* **89**, 447-454 (2016).

[25] D. Baleanu, A. Jajarmi and M. Hajipour, A new formulation of the fractional optimal control problems involving Mittag-Leffernon-singular kernel, *J. Optim. theory Appl.* **175**(3), 718-737 (2017).

[26] B. P. Belousov, Collection of short papers on radiation medicine for 1958, Medgiz:Moscow, 145-147 (1959).

[27] M. Zhabotinsky, Periodic oxidation of malonic acid in solution(a study of the Belousov reaction kinetics), *Biofizika* **9**, 306-311 (1964).

[28] R. J. Field, E. Körös and R. M Noyes, Oscillations in chemical systems II thorough analysis of temporal oscillation in the bromatecerium-malonic acid system, *J. Am. Chem. Soc.* **94**, 8649-8664 (1972).

[29] R. J. Field and R. M. Noyes, Oscillations in chemical systems. IV. limit cycle behavior in a model of a real chemical reaction, *J. Chem. Phys.* **60**, 1877-1884 (1974).

[30] Q. Wang, Numerical solutions for fractional KdV-burgers equation by Adomian decomposition method, *Appl. Math. Comput.* **182**, 1048-1055 (2006).

[31] Z. Odibat and S. Momani, The variational iteration method: An efficient scheme for handling fractional partial differential equations in fluid mechanics, *Comput. Math. Appl.* **58**, 2199-2208 (2009).

[32] N. Sweilam, M. Khader and R. Al-Bar, Numerical studies for a multi-order fractional differential equation, *Phys. Lett. A* **371**, 26-33 (2007).

[33] I. Hashim, O. Abdulaziz and S. Momani, Homotopy analysis method for fractional ivps, Commun. *Nonlin. Sci. Numer. Simul.* **14**, 674-684 (2009).

[34] S. Abuasad, I. Hashim and S. A. A. Karim, Modified fractional reduced differential transform method for the solution of multiterm time-fractional diffusion equations, *Adv. Math. Phys.*, (2019). DOI: 10.1155/2019/5703916.

[35] K. Diethelm, N. J. Ford and A. D. Freed, A predictor corrector approach for the numerical solution of fractional differential equations, *Nonlin. Dyn.* **29**(1), 3-22 (2002).

[36] A. Jafarian, M. Mokhtarpour and D. Baleanu, Artificial neural network approach for a class of fractional ordinary differential equation, *Neural. Comput. Appl.* **28**(4), 765-773 (2017).

[37] C. Baishya, An operational matrix based on the Independence polynomial of a complete bipartite graph for the Caputo fractional derivative, *SeMA J.*, (2021).
[38] S. J. Achar, C. Baishya and M. K. A. Kaabar, Dynamics of the worm transmission in wireless sensor network in the framework of fractional derivatives, *Math. Meth. Appl. Sci.* **45**(8), 4278-4294 (2022).
[39] S. Kazem, S. Abbasbandy and S. Kumar, Fractional-order legendre functions for solving fractional-order differential equations, *Appl. Math. Model.* **7**(37), 5498-5510 (2013).
[40] S. J. Liao, Homotopy analysis method: a new analytic method for nonlinear problems, *Appl. Math. Mech.* **19**, 957-962 (1998).
[41] J. Singh, D. Kumar and R. Swroop, Numerical solution of time- and space-fractional coupled Burgers' equations via homotopy algorithm, *Alexandria Eng. J.* **55** (2), 1753-1763 (2016).
[42] H. M. Srivastava, D. Kumar and J. Singh, An efficient analytical technique for fractional model of vibration equation, *Appl. Math. Model.* **45**, 192–204 (2017).
[43] D. Kumar, R. P. Agarwal and J. Singh, A modified numerical scheme and convergence analysis for fractional model of Lienard's equation, *J. Comput. Appl. Math.* **399**, 405-413 (2018).

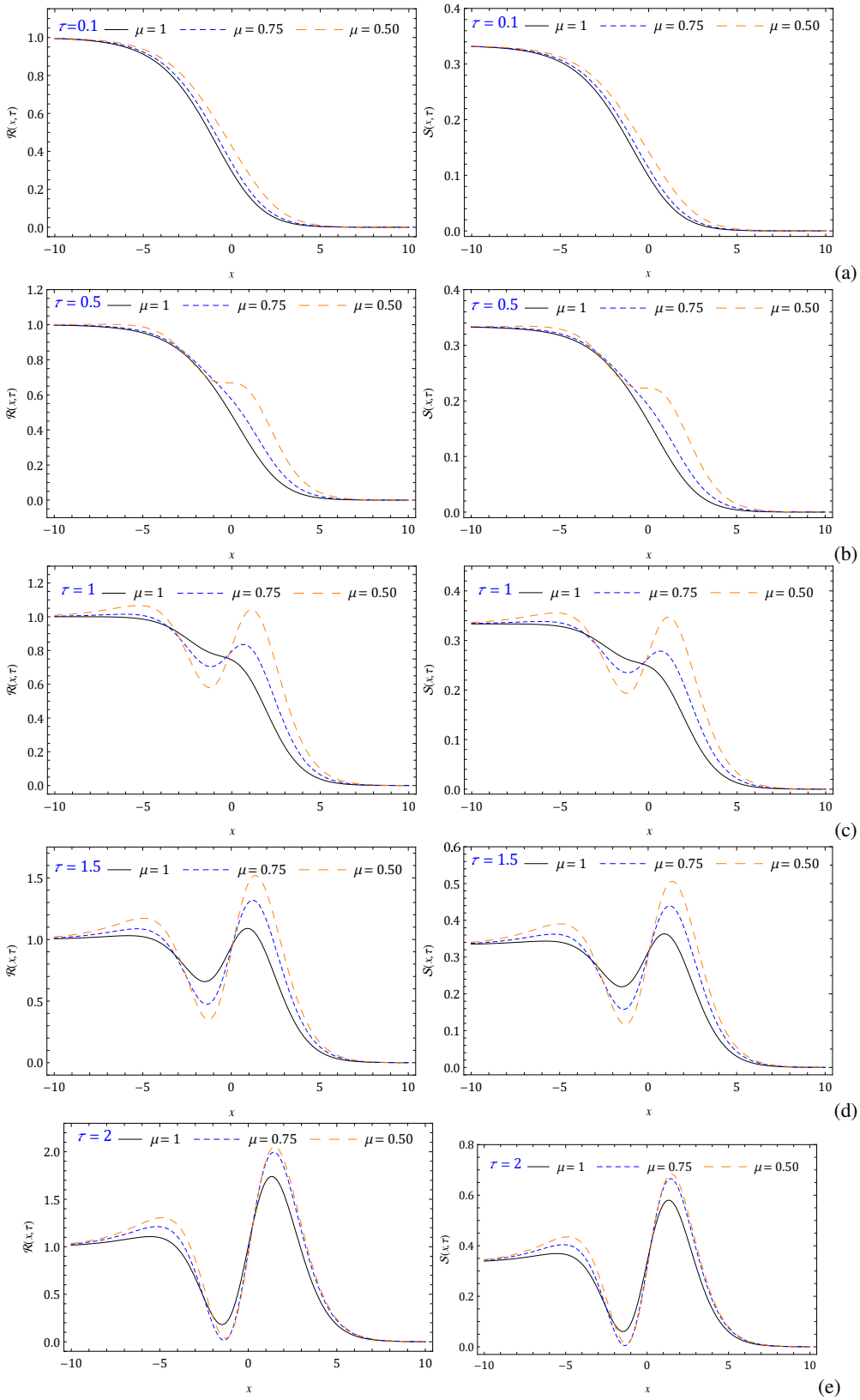

Fig. 2: Nature of the obtained solution for Example 1 at $(a)\,\tau = 0.1,\ (b)\,\tau = 0.5,\ (c)\,\tau = 1,\ (d)\,\tau = 1.5$ and $(e)\,\tau = 2$ with distinct μ with $\alpha = 2,\ \hbar = -1,\ n = 1$ and $\beta = 3$ for $\mathscr{R}(\varkappa, \tau)$ and $\mathscr{S}(\varkappa, \tau)$.

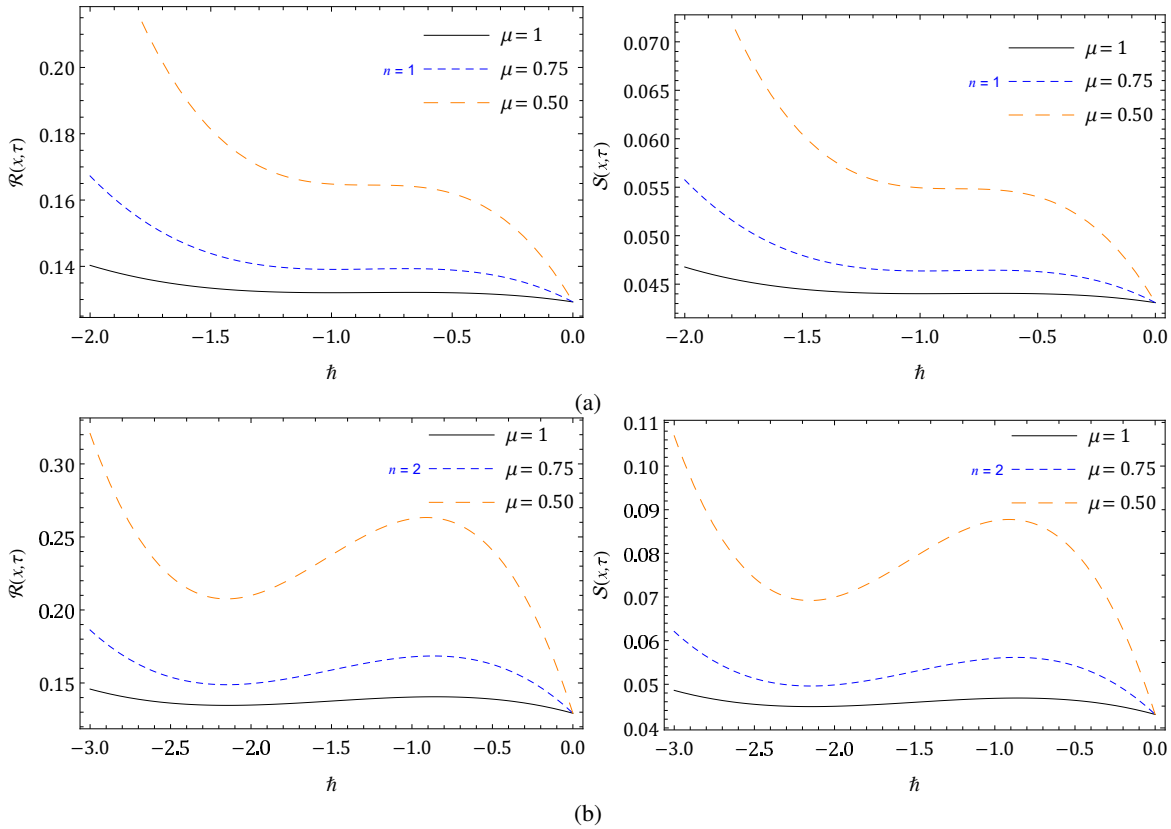

Fig. 3: $\hbar$-curves for $(a)\mathscr{R}(\varkappa,\tau)$, $(b)\mathscr{S}(\varkappa,\tau)$ of Example 1 with distinct μ at $\alpha = 2,\ \beta = 3,\ \varkappa = 1$ and $\tau = 0.01$ with $n = 1$ and 2.

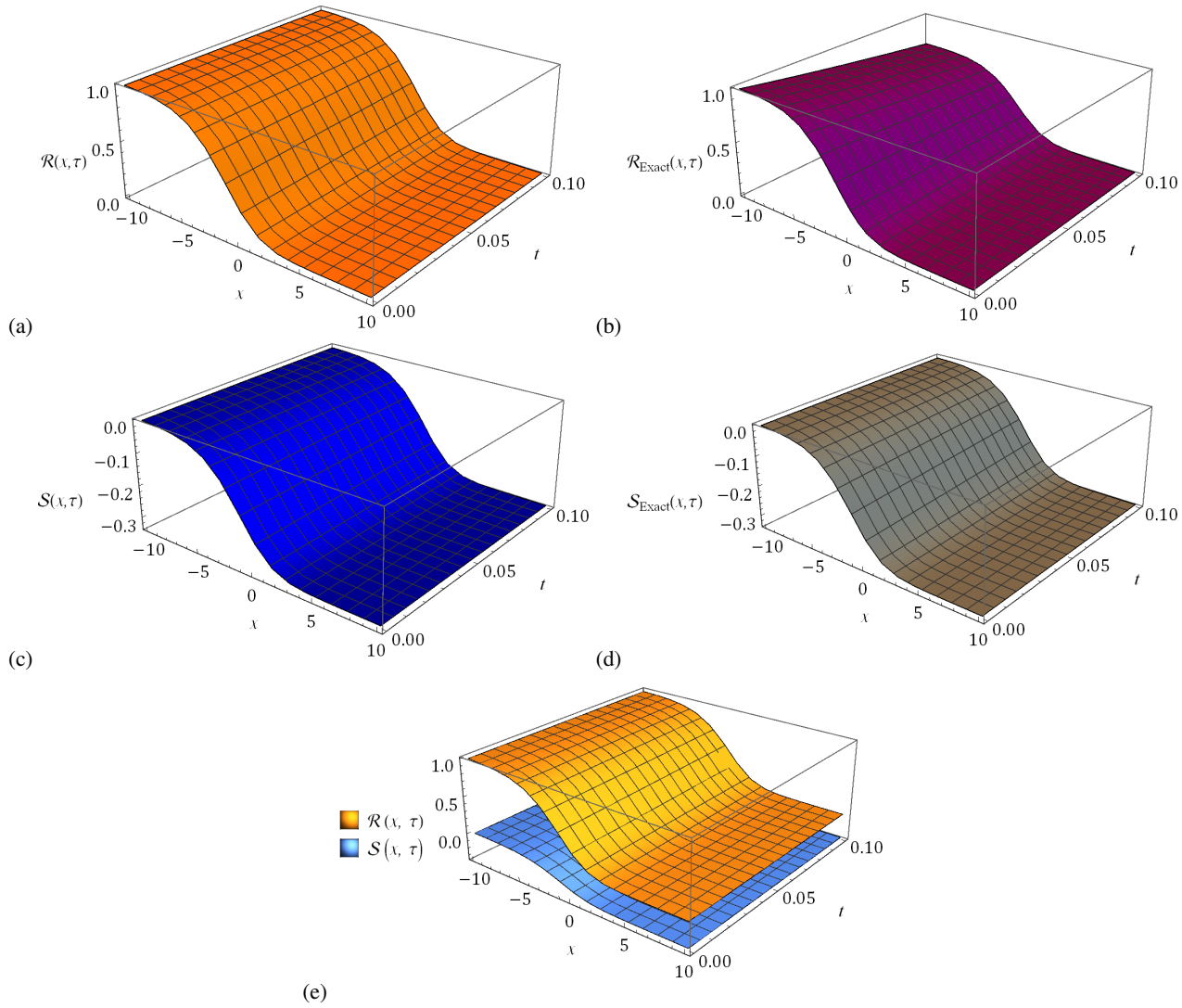

Fig. 4: Surfaces of $(a)\mathscr{R}_{q-HATM}, (b)\mathscr{R}_{Exact}, (c)\mathscr{S}_{q-HATM}, (d)\mathscr{S}_{Exact}, (e)$ coupled surface at $\alpha = 2, \beta = 3,\ \hbar = -1,\ n = 1$ and $\mu = 1$ for Example 2.

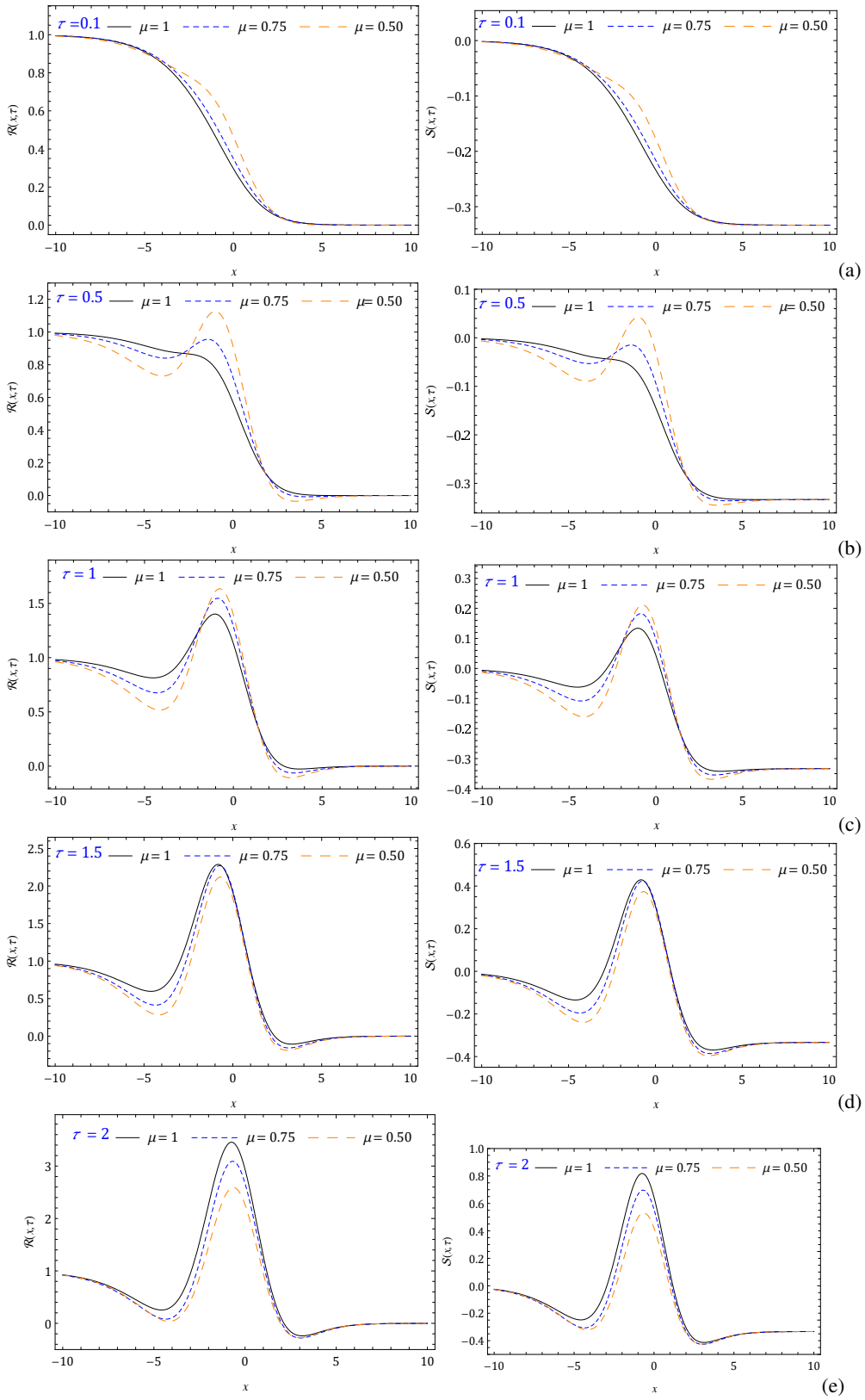

Fig. 5: Nature of the obtained solution for Example 2 at $(a)\tau = 0.1,\ (b)\tau = 0.5,\ (c)\tau = 1,\ (d)\tau = 1.5$ and $(e)\tau = 2$ with distinct μ with $\alpha = 2,\ \hbar = -1,\ n = 1$ and $\beta = 3$ for $\mathscr{R}(\varkappa,\tau)$ and $\mathscr{S}(\varkappa,\tau)$.

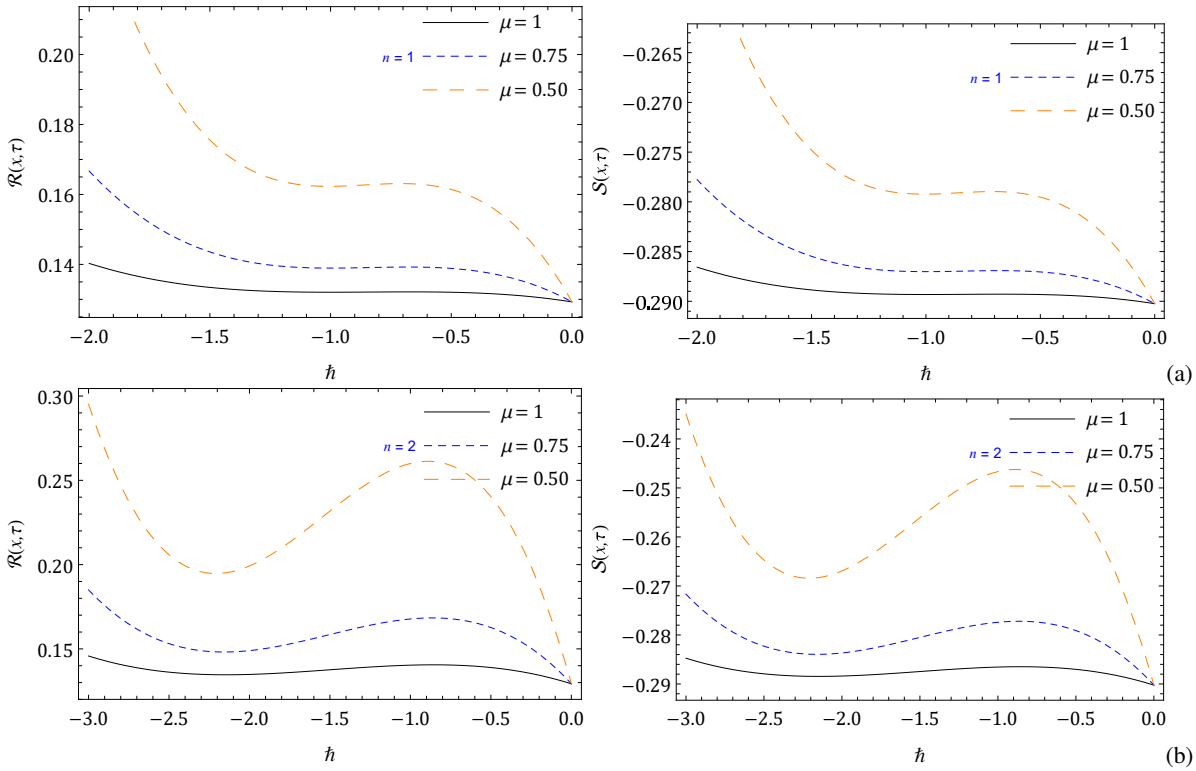

Fig. 6: $\hbar$-curves for $(a)\mathscr{R}(\varkappa,\tau)$, $(b)\mathscr{S}(\varkappa,\tau)$ of Example 2 with distinct μ at $\alpha = 2,\ \beta = 3,\ \varkappa = 1$ and $\tau = 0.01$ with $n = 1$ and 2.